

〈Original Article〉

## Left ventricular mechanics and myocardial calcium dynamics in short-term and long-term hyperthyroid mice

Yumi SASAE<sup>1, 2)</sup>, Ken HASHIMOTO<sup>1)</sup>, Yoshihiro UJIHARA<sup>1)</sup>,  
Akira HANASHIMA<sup>1)</sup>, Takeshi HONDA<sup>1)</sup>, Yoshitaka MORITA<sup>2)</sup>,  
Satoshi MOHRI<sup>1)</sup>

*1) Department of Physiology 1, 2) Department of Rheumatology,  
Kawasaki Medical School, 577 Matsushima, Kurashiki, 701-0192, Japan*

**ABSTRACT** The thyroid hormone is involved in cardiac adaptation to physiological and pathological stimuli. Although short-term hyperthyroidism enhances cardiac performance, longstanding hyperthyroidism can cause impairment of the contractility by pathological  $\text{Ca}^{2+}$  handling. Because the thyroid hormone affects cardiovascular hemodynamics by decreasing systemic arterial resistance and increasing circulating blood volume, it is important to accurately analyze left ventricular (LV) mechanics by using an index that is independent of ventricular loading conditions. Therefore, we adopted the end-systolic elastance ( $E_{es}$ ), which is obtained by the linear regression of the end-systolic pressure-volume relationships. This reflects sensitive changes in the contractile state in a manner independent of both preload and afterload, providing an index of LV contractility. To better understand the hypertrophy caused by hyperthyroidism, we normalized the  $E_{es}$  according to LV weight for different sized heart. Hyperthyroidism was induced by a daily intraperitoneal injection of triiodothyronine (T3) at a dose of 2,000 mg/kg body weight. Mice were divided into three groups: the synchronous control group, the T3 administration for one-week group (T3-short), and the T3 administration for eight-week group (T3-long). We investigated global LV mechanics, the expression of  $\text{Na}^+/\text{Ca}^{2+}$  exchanger (NCX), the sarco/endoplasmic reticulum  $\text{Ca}^{2+}$ -ATPase (SERCA), and the  $\text{Ca}^{2+}$  handling of isolated cardiomyocytes in each group.  $E_{es}$  values in the control and T3-short were similar, and those in T3-long were significantly smaller than the control ( $256 \pm 60$ ,  $249 \pm 70$  and  $154 \pm 57$  mmHg·ml<sup>-1</sup>·gLV<sup>-1</sup>, respectively). The values of arterial elastance in both T3-short and T3-long, which represent afterload, were significantly smaller than the control. NCX expression was decreased in T3-short and declined in a time-dependent manner in T3-long. On the other hand, SERCA expression was rapidly elevated in T3-short and remained high in T3-long. These changes may be beneficial for cardiomyocytes in terms of  $\text{O}_2$  consumption for excitation-contraction coupling. In isolated cardiomyocyte experiments,

---

Corresponding author  
Satoshi Mohri  
Department of Physiology 1, Kawasaki Medical School,  
577 Matsushima, Kurashiki, 701-0192, Japan

Phone : 81 86 462 1111  
Fax : 81 86 462 1121  
E-mail: smohri@med.kawasaki-m.ac.jp

cell shortening of T3-long mice was significantly lower than that of the control mice, but the average peak amplitude of  $\text{Ca}^{2+}$  transients in T3-long was 79% and not significantly different. In conclusion, we evaluated LV contractility by using an Ees index in hyperthyroid mice. Although T3 administration shifted the  $\text{Ca}^{2+}$  route in excitation-contraction coupling to the  $\text{O}_2$ -saving energetics, LV contractility was diminished with long-term T3 administration, showed constancy in peak amplitude of the  $\text{Ca}^{2+}$  transients, and a decrease in NCX activity.

doi:10.11482/KMJ-E41(2)41 (Accepted on October 6, 2015)

Key words : Cardiac hypertrophy, Contractility, Mice, Sodium-calcium exchanger, Sarcoplasmic reticulum  $\text{Ca}^{2+}$  ATPase

## INTRODUCTION

The thyroid hormone affects cardiac function by regulating many factors in the myocardium, such as calcium handling<sup>1)</sup>, shape and geometry<sup>2)</sup>, and electrophysiological function<sup>3, 4)</sup>. Clinically, hyperthyroidism results in enhanced cardiac contractility and relaxation subsequently causes congestive heart failure. One possible mechanism behind the transition of the initial adaptive response to decompensation can be tachycardia, which increases myocardial intracellular calcium. It has been reported that suppression of the heart rate did not completely prevent myocardial hypertrophy and subsequent deterioration of the cardiac function<sup>5)</sup>. Therefore, there must be other reasons why longstanding hyperthyroidism causes heart failure.

Calcium is a significant factor not only in the regulation of excitation-contraction coupling but also in the development of cardiac hypertrophy and heart failure<sup>6)</sup>. One critical calcium-related molecular mechanism of cardiac hypertrophy is calcineurin signaling, which regulates the translocation of the transcription factor nuclear factor of activated T-lymphocyte-3 to the nucleus through calcium-dependent dephosphorylation<sup>7)</sup>. The calmodulin-dependent protein kinase also plays an important role in regulating cardiac hypertrophy in a calcium-dependent manner<sup>8)</sup>.

In myocardium, calcium is handled by various

calcium transport proteins in the sarcoplasmic reticulum and plasma membrane, such as L-type calcium channel (LTCC),  $\text{Na}^+/\text{Ca}^{2+}$  exchanger (NCX), ryanodine receptor 2 (RYR-2), and sarco/endoplasmic reticulum  $\text{Ca}^{2+}$ -ATPase (SERCA). These  $\text{Ca}^{2+}$  transporters play a pivotal role in excitation-contraction coupling (E-C coupling), and there are two major  $\text{Ca}^{2+}$  handling routes. One is the route recirculating  $\text{Ca}^{2+}$  intracellularly via the sarcoplasmic reticulum (SR), and the other is the route entering  $\text{Ca}^{2+}$  via LTCC and extruding  $\text{Ca}^{2+}$  by NCX. Since these intracellular (internal) and transsarcolemmal (external) handlings have different molecular  $\text{Ca}^{2+}$  ATPase stoichiometries, regulation of  $\text{Ca}^{2+}$  transporters may be very important to maintain cardiac function. Although an antithetical regulation of NCX and SERCA in short-term hyperthyroidism has been reported<sup>1)</sup>, calcium dynamics in the thyroid hormone-induced failing of the myocardium have not been investigated.

Cardiovascular hemodynamics are also significantly affected by the thyroid hormone. Direct effects on vascular smooth muscle cells at arterioles decrease systemic arterial resistance<sup>9)</sup>. The thyroid hormone also activates the rennin-angiotensin-aldosterone system and increases renal sodium reabsorption, resulting in an increase in circulating blood volume<sup>10)</sup>. Therefore, it may be insufficient to characterize the effects of the thyroid hormone on cardiac pump function with conventional,

preload- (circulating blood volume), and afterload- (systemic arterial resistance) dependent cardiac parameters. The end-systolic elastance (Ees), which is obtained from the linear regression of the end-systolic pressure-volume relationships (ESPVRs), reflects sensitive changes in the contractile state in a manner independent of ventricular loading conditions<sup>11</sup>. Moreover, the hyperthyroidism causes cardiac hypertrophy and changes the heart size. When we compare cardiac contractility between different sized hearts, Ees must be normalized with respect to the heart size because the Ees of a smaller heart tends to be greater than that of a larger heart. One method of normalizing Ees for different sized hearts is dividing ventricular end-systolic volume by ventricular wall weight and then dividing ventricular end-systolic pressure by this normalized volume<sup>11</sup>. Using this normalizing method, we succeeded in accurately evaluating ventricular mechanics in hyperthyroid mice in different cardiac states.

In this study, we evaluated the left ventricular (LV) mechanics using Ees, which is practically load-independent and normalized by LV weight and corresponding NCX and SERCA expression, and the intracellular calcium dynamics of isolated cardiomyocytes in short-term and long-term hyperthyroid mice.

## MATERIALS AND METHODS

### *Animals*

Experiments were performed on male C57/BL6J mice aged 8-week old (weighing 22-24 g). Hyperthyroidism was induced by daily intraperitoneal injections of T3 (2,000 mg/kg body weight). Mice were divided into three groups: the synchronous control group, the T3 administration for 1 week group (T3-short), and the T3 administration for 8 weeks group (T3-long). T3 was purchased from Sigma (St. Louis, USA). All procedures in this study were approved by the Kawasaki Medical School Institutional Review Board.

### *Surgical preparation*

The part of left ventricular pressure and volume study was performed in 15 mice (n = 5 each group). Mice were anesthetized with sevoflurane (2-5%) and intubated. They were mechanically ventilated using a volume-controlled ventilator (SN-480-7 Shinano) with tidal volume 200 ml and respiratory rate 120 breath/min. The diaphragm was opened via an abdominal incision and the pericardium was dissected to expose the heart. After soaking in saline for 30 minutes to hydrate the sensor properly, we introduced a 1.2 Fr conductance catheter (ADVantage™ 5.0, Scisense Inc.) into LV through an apical stab made by the puncture using 27G needle to measure the LV volume and pressure. The distal electrode of the catheter was positioned carefully at the level of the aortic valve and the proximal electrode near the apex. A 4-0 suture was placed loosely around the inferior vena cava for occlusion (IVCO) to decrease the LV preload (end-diastolic volume).

### *Experimental protocol and data analysis in LV mechanics*

After completion of the surgical preparation, steady-state LV pressure and volume signals were recorded. Subsequently, the signals during IVCO (~5 sec) were recorded. Concentration of sevoflurane was controlled to keep the heart rate  $500 \pm 20$  beats/min. The ventilator was stopped during data acquisition to avoid respiratory fluctuation of cardiac signals.

The end-systolic pressure-volume relationships (ESPVRs) were obtained from the data during IVCO in the usual fashion<sup>12</sup> and analyzed by linear regression to obtain the LV contractility index end-systolic elastance (Ees). In this study, we tried to compare the cardiac contractility among the LVs of different sizes because thyroid hormone caused LV hypertrophy. Therefore we adopted the method of normalizing the Ees (n-Ees) for different sized

heart that was to divide LV volume by LV weight as reported previously<sup>13</sup>. Ejection fraction (EF) was calculated as  $100 \cdot (\text{EDV} - \text{ESV}) / \text{EDV}$ , where EDV and ESV are the end-diastolic and end-systolic LV volume, respectively. To evaluate the LV afterload, we obtained arterial elastance ( $E_a$ ) by calculating the ratio of end-systolic pressure to stroke volume ( $\text{SV}$ )<sup>14</sup>. It has been recognized that systemic vascular resistance (SVR) decreases in hyperthyroidism. SVR is obtained by dividing the mean aortic pressure by the cardiac output; therefore, the unit of SVR is  $\text{mmHg}/\text{min}/\text{mL}^{-1}$ .  $E_a$  is synonymous with SVR, and its unit is  $\text{mmHg}/\text{mL}^{-1}$ . Inotropic and lusitropic properties were also evaluated by determining maximum (+max  $dP/dt$ ) and minimum (-max  $dP/dt$ ) rate of pressure change and the time constant of pressure decay during relaxation as indexed by the logistic time constant ( $\tau_L$ )<sup>15</sup>. For calculation of  $\tau_L$ , we analyzed the time constant of isovolumic relaxation from the time of peak  $-dP/dt$  to the time when LVP fell to 5 mmHg above the EDP using a least-squares method performed in Kaleida Graph (Synergy software).

#### *Immunoblotting*

Hearts were collected from mice and snap frozen in liquid nitrogen. Minced tissues were homogenized using Polytron homogenizer (PT1600E, Kinematica) or MicroSmash homogenizer (MS-100R, Tomy, Japan) in one of the following lysis buffer: 10mM Tris-HCl; pH7.5, 150mM NaCl, 0.5mM EDTA, 10mM NaF, and 0.5% Triton X-100, M-PER Mammalian Protein Extraction Reagent (Thermo Scientific), or cytoplasmic extraction buffer from Subcellular Protein Fractionation Kit (Thermo Scientific) in the presence of protease and phosphatase inhibitor cocktail (Thermo Scientific or Roche). Lysates were centrifuged at 14,000 g for 10 min and supernatants were used for immunoblot analysis. After quantifying total protein concentrations by bicinchoninic acid (BCA)

method, equal amount of proteins were loaded on 4%-15% SDS-PAGE gradient gels (Bio Rad), separated, and transferred onto polyvinylidene difluoride (PVDF) membranes (GE Healthcare). After blocking the membranes with 3% BSA in TBS-T, they were probed with primary antibodies for NCX (1:3000 dilution, anti-NCX antibody was a kind gift from Dr. Yuki Katanosaka, Okayama University, Japan<sup>16</sup>) or SERCA (1:1000 dilution, MA3-919, Thermo Scientific). The membranes were then probed with secondary horseradish peroxidase (HRP)-conjugated IgG (GE Healthcare), and finally visualized by enhanced chemiluminescence (Western Lightning ECL-Pro, PerkinElmer) using LAS4000mini luminescent image analyzer (Fuji Film). Densitometry analysis was performed using Image J software.

#### *qPCR*

Hearts were collected from mice, cut into small pieces, and immediately immersed in RNAlater RNA Stabilization Reagent (Qiagen). The stabilized tissues were homogenized with MicroSmash homogenizer (MS-100R, Tomy, Japan), and total RNA was isolated using RNeasy Fibrous Tissue Mini Kit (Qiagen). After assessing RNA yield and quality by NanoDrop spectrophotometer (ND-1000, Thermo Scientific), RNA samples were reverse-transcribed with PrimeScrip RT Master Mix (Takara), and quantitative PCR was performed with TaqMan Fast Advanced Master Mix in a StepOnePlus real time PCR system (Applied Biosystems) for thyroid hormone receptor  $\alpha$  (Thra, Mm00579691\_m1, Applied Biosystems). Quantification of Thra mRNA was carried out with Rn18S (Mm03928990\_g1, Applied Biosystems) as the reference gene using the  $\Delta\Delta C_T$  method.

#### *Isolation of adult mouse ventricular myocytes*

Single cardiomyocytes were enzymatically isolated from mice in a similar method to previous

studies<sup>17,18</sup>). Firstly, hearts were rapidly removed from the mice anesthetized with an overdose of 300 mg/kg pentobarbital, *i.p.*, and then Langendorff-perfused for 3-4 min at 37 °C using cell isolation buffer (CIB: 130 mM NaCl, 5.4 mM KCl, 0.5 mM MgCl<sub>2</sub>, 0.33 mM NaH<sub>2</sub>PO<sub>4</sub>, 22 mM glucose, 50 nM/ml bovine insulin (Sigma) and 25 mM HEPES-NaOH (pH 7.4.)) supplemented with 0.4 mM EGTA (EGTA-CIB). Then, the perfusate was switched to enzyme solution (CIB containing with 1 mg/ml collagenase (Worthington Biochemical), 0.06 mg/ml trypsin (Sigma) and 0.06 mg/ml protease (Sigma)) supplemented with 0.3 mM CaCl<sub>2</sub>. After 6-9 min, the left ventricular tissue was excised from the digested heart, and it was cut into several pieces and further digested in 10 ml fresh enzyme solution supplement with 0.7 mM CaCl<sub>2</sub> and 2 mg/ml BSA (Sigma) for 15-20 min at 37 °C. The cell suspension was centrifuged at 14 × g for 5 min and the cell pellet was resuspended in CIB supplemented with 1.2 mM CaCl<sub>2</sub> and 2 mg/ml BSA, and then incubated at 37 °C for 10 min. Following centrifugation, finally, the cell pellet was resuspended in standard Tyrode's solution (140 mM NaCl, 5.4 mM KCl, 1.8 mM CaCl<sub>2</sub>, 0.5 mM MgCl<sub>2</sub>, 0.33 mM NaH<sub>2</sub>PO<sub>4</sub>, 11 mM glucose, 2 mg/ml BSA and 5 mM HEPES-NaOH (pH 7.4)).

#### *Measurements of cell shortenings and intracellular Ca<sup>2+</sup> transients in cardiomyocytes*

Cell shortenings and intracellular Ca<sup>2+</sup> transients induced by electronic stimulations were measured as previously described<sup>18,19</sup>. Isolated cells were electrically stimulated at 1 Hz in standard Tyrode's solution using a two-platinum electrode insert connected to a bipolar stimulator (SEN-3301, Nihon Kohden). They were examined using an inverted microscope (IX71, Olympus) with a 20 × water immersion objective lens (UApo N340, Olympus). Images were acquired using a High-performance EvolveTM EMCCD camera (Photometrics) and

obtained images were analyzed using MetaMorph software (Molecular Devices).

#### *Measurements of intracellular Ca<sup>2+</sup>*

Indo-1 AM (Dojindo) was used for the measurements of Ca<sup>2+</sup> transients evoked by electronic stimulation at 1 Hz. Isolated cells were loaded with 10 μM indo-1 AM for 10 min at 37 °C. Cells loaded with Indo-1 AM were examined in standard Tyrode's solution using the same experimental apparatus as the measurement of cell shortenings. Cells were excited with 340 nm with emissions of 405 and 485 nm. Ca<sup>2+</sup> transients were measured as the difference of the 405/480 ratio from basal levels. To evaluate the decay speed after peak Ca<sup>2+</sup> transients, the time constant was calculated by fitting a mono-exponential curve to the decay of the normalized Ca<sup>2+</sup> transient (from 90% to 10% amplitude). Fura-2 AM (Dojindo) was used as an intracellular indicator of Ca<sup>2+</sup> for the measurement of NCX activity and SR Ca<sup>2+</sup> content. Isolated cells were loaded with 5 μM Fura-2 AM for 30 min at 37 °C. Cells were studied using an inverted IX71 microscope (Olympus) with a UApo 20 × /0.75 objective lens (Olympus). Cells were excited at 340 and 380 nm using a Lambda DG-4 Ultra High Speed Wavelength Switcher (Sutter Instruments) and the fluorescent emissions (F340 and F380) were recorded with ORCA-Flash 2.8 (Hamamatsu Photonics) analyzed by a ratiometric fluorescence method using MetaFluor software (Molecular Devices) as previously described<sup>20</sup>. The signal was expressed as the ratio (F340/F380) of the emissions at those excitation wavelengths.

#### *Measurements SR Ca<sup>2+</sup> contents*

SR Ca<sup>2+</sup> content was measured as Ca<sup>2+</sup> increase induced by caffeine. After cells loaded with Fura-2 were electrically stimulated until Ca<sup>2+</sup> transients reached steady-state, 10 mM caffeine was rapidly applied. Peak amplitude of a caffeine-induced Ca<sup>2+</sup>

transient was taken as an index of SR  $\text{Ca}^{2+}$  content.

#### *Measurements of NCX activity*

NCX activity in cells was measured as intracellular  $\text{Na}^+$ -dependent  $\text{Ca}^{2+}$  uptake by a modification of previously describes<sup>16</sup>. Following Fura-2 loading, cells were loaded with  $\text{Na}^+$  by incubating them at 37 °C for 15 min in normal BSS (10mM Hepes/Tris (pH7.4), 146 mM NaCl, 4 mM KCl, 2 mM  $\text{MgCl}_2$ , 0.1 mM  $\text{Ca}_2\text{Cl}$ , 10 mM glucose, and 0.1% BSA) containing 1  $\mu\text{M}$  ouabain, 1  $\mu\text{M}$  thapsigargin and 1  $\mu\text{M}$  monensin. After  $\text{Na}^+$  loading, the cells were washed in normal BSS containing 1  $\mu\text{M}$  ouabain, 1  $\mu\text{M}$  thapsigargin, 5  $\mu\text{M}$  nifedipine.  $\text{Ca}^{2+}$  uptake was performed by perfusing the cells with  $\text{Na}^+$ -free (choline chloride<sup>+</sup> containing) BSS containing 1  $\mu\text{M}$  ouabain, 1  $\mu\text{M}$  thapsigargin, 5  $\mu\text{M}$  nifedipine. NCX activity was evaluated by calculating the slope of the line obtained by linear regression analysis of the relationship between Fura-2 ratio and time for first 20 s after medium switching.

#### *Immunofluorescence microscopy*

Excised hearts were immediately embedded in OCT compound (Tissue-Tek) and were frozen. Frozen heart blocks were sectioned to a thickness of 5  $\mu\text{m}$ . The sections were washed with phosphate-buffered saline (PBS) and permeabilized with PBS containing 0.1% Triton X-100 for 5 min. The sections were then immersed in Block-One (Nacalai Tesque) for 30 min to block non-specific binding, and were incubated with the primary antibody against NCX1 for 1h at 4 °C. The sections were washed with PBS containing 0.1% Tween 20 (PBS-T) and then they were exposed to Alexa Fluor 488-conjugated anti-rabbit IgG antibody (Life Technologies) in PBS-T for 15 min. After the sections were washed with PBS-T, nuclei stained with DAPI (Life Technologies) in PBS-T for 5 min at 4 °C. The sections were washed with PBS-T again, and they were mounted with Dako fluorescent

mounting medium (DAKO). The fluorescently stained sections were observed under a confocal laser scanning microscope (FV1000, Olympus) with a UPlanApo  $\times 60/1.35$  oil immersion objective lens (Olympus).

#### *Statistics*

Results are presented as mean  $\pm$  SEM but presented as mean  $\pm$  SD in variables of LV mechanics in Table. They were analyzed by one-way analysis of variance (ANOVA) followed by Dunnett's test for comparison against a control group. *P* values of less than 0.05 were considered statistically significant.

## **RESULTS**

#### *LV mechanics*

Representative steady-state tracings of LV pressure, pressure-volume loops and variables of cardiac mechanics are shown in Fig. 1 and table. Both EDV and LV weight significantly increased in T3-long compared with control. n-EDV, the quotient of EDV and LV weight, significantly increased in T3-short and T3-long, indicating that the lumen-to-wall ratio at end-diastole was increased by T3 administration. Peak LV pressure in T3-long was significantly lower compared with that of control. There was no significant difference in cardiac contractility Ees between the control and T3-short. In T3-long, there was a rightward shift of the ESPVR (decreased contractility; Fig. 1B, D, and F), and Ees decreased significantly.

The values of  $E_a$  in T3-short and T3-long were significantly smaller than the control, indicating that the LV afterload was decreased by T3. Greater EF in T3-short than that in the control can be explained by similar contractility and a lower LV afterload in T3-short. On the other hand, diminished contractility resulted in lower EF despite a decreased LV afterload in T3-long. Using Ees, which is a preload and afterload independent index of ventricular

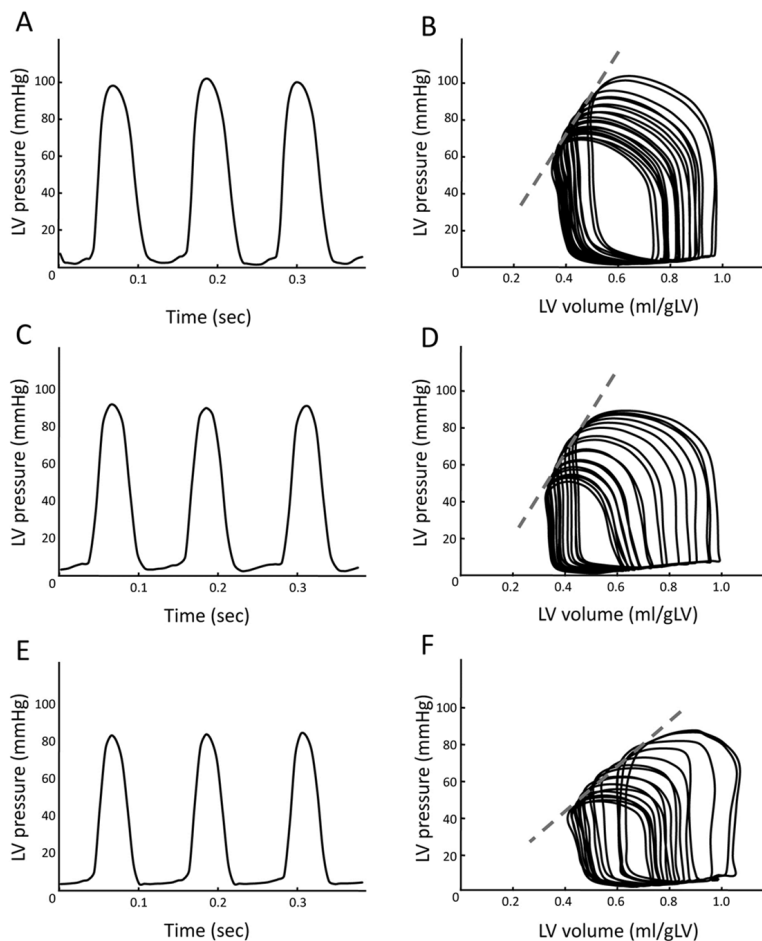


Fig. 1. Representative set of left ventricular pressure curves (left) and pressure-volume loops (right) during inferior vena cava occlusion of control (upper), T3-short (middle) and T3-long (lower). Broken lines show the end-systolic pressure-volume relationship and their slopes are Ees representing ventricular contractility (B, D and F).

Table. Variables of LV mechanics in each group

Variable	Control (n = 5)	T3-short (n = 5)	T3-long (n = 5)
EDV ( $\times 10^{-3}$ ml)	69.6 $\pm$ 13.5	93.0 $\pm$ 22.7	123 $\pm$ 32.9*
Peak LV Pressure (mmHg)	105 $\pm$ 8.4	99 $\pm$ 7.3	84 $\pm$ 7.3*
LV weight ( $\times 10^{-3}$ g)	77.8 $\pm$ 8.93	84.6 $\pm$ 7.40	107 $\pm$ 11.6*
n-EDV (ml $\cdot$ gLV $^{-1}$ )	0.913 $\pm$ 0.245	1.11 $\pm$ 0.304*	1.14 $\pm$ 0.212*
Ees (mmHg $\cdot$ ml $^{-1}$ $\cdot$ gLV $^{-1}$ )	256 $\pm$ 60	249 $\pm$ 70	154 $\pm$ 57*
EF (%)	51.8 $\pm$ 8.35	55.8 $\pm$ 10.5*	38.8 $\pm$ 12.4*
Ea (mmHg $\cdot$ ml $^{-1}$ )	2.52 $\pm$ 0.55	1.70 $\pm$ 0.31*	1.54 $\pm$ 0.35*
+max dP/dt (mmHg $\cdot$ s $^{-1}$ )	7238 $\pm$ 663	7683 $\pm$ 371	7825 $\pm$ 428
-max dP/dt (mmHg $\cdot$ s $^{-1}$ )	6910 $\pm$ 732	7526 $\pm$ 402	7665 $\pm$ 440
$\tau_L$ (ms)	9.88 $\pm$ 1.70	9.18 $\pm$ 1.18	7.68 $\pm$ 1.08*

Each value indicates mean  $\pm$  SD. Ees, end-systolic elastance; EDV, end-diastolic volume; LV pressure, left ventricular pressure; n-EDV, EDV normalized for 1 g LV weight; EF, ejection fraction; Ea, arterial elastance; +max dP/dt, maximum positive value of time derivative of LV pressure; -max dP/dt, maximum negative value of time derivative of LV pressure;  $\tau_L$ , time constant of isovolumic relaxation pressure segment after -max dP/dt. Statistically significant difference at \*:  $p < 0.05$  compared with control.

contractility, we could evaluate cardiac performance per se under different conditions of arterial resistance and circulating blood volume. As for the pressure-derived indices,  $\tau_L$  in T3-long was significantly smaller than the control, and there were no significant differences in either +max dP/dt or -max dP/dt (Table, Fig. 1A, C, and E).

#### Immunoblotting

As shown in Fig. 2, NCX1 protein expression decreased after T3 administration for one week (T3-short), and it further declined in a time-dependent manner with long-term administration (T3-long). On the other hand, the expression level of SERCA2 rapidly elevated with one week of T3 administration, and it remained high with the long-term administration.

#### $Ca^{2+}$ measurements in isolated cardiomyocytes

To understand the effects of T3 on cardiomyocytes, we analyzed cell morphology and shortening in cardiomyocytes that were isolated from hearts in the control, T3-short and T3-long mice. Cells isolated from T3-short mice were rod-shaped, as were those of the control, although the projected area was increased (Fig. 3A and C). Cell shortening of T3-short was almost the same level as that of the control (Fig. 3B). By contrast, the cells in T3-long mice showed an irregular structure with a significantly increased projected area (Fig. 3A and C). Cell shortening of T3-long mice showed significantly lower than that of control (Fig. 3B). Thus, the mice treated with T3 for a long time showed abnormal morphology and impaired contractility at the single cell level.

We further investigated how T3 administration

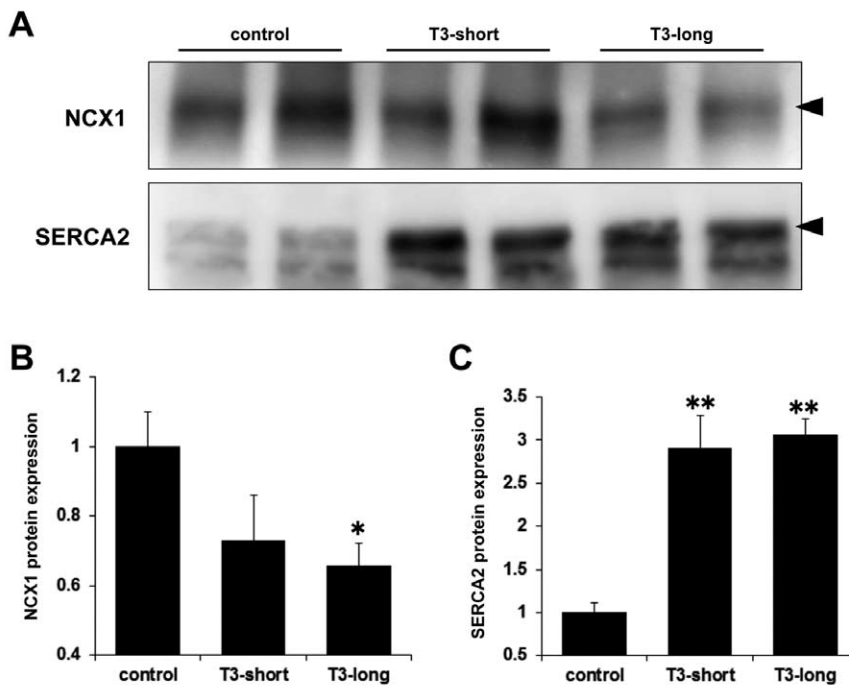


Fig. 2. (A) Whole (cytoplasmic) protein extracts were obtained from adult mouse hearts (control, T3-short, and T3-long), and analyzed by western blotting for NCX (B) and SERCA (C). \*  $P < 0.05$ , \*\*  $P < 0.01$  vs. control group by one-way analysis of variance followed by Dunnett's post hoc test. Data were normalized to the control level which was set at 1 and expressed as mean plus SEM.  $n = 4, 4,$  and  $6$  mice for control, T3-short, and T3-long, respectively for NCX.  $n = 6, 5,$  and  $4$  mice for control, T3-short, and T3-long, respectively for SERCA.

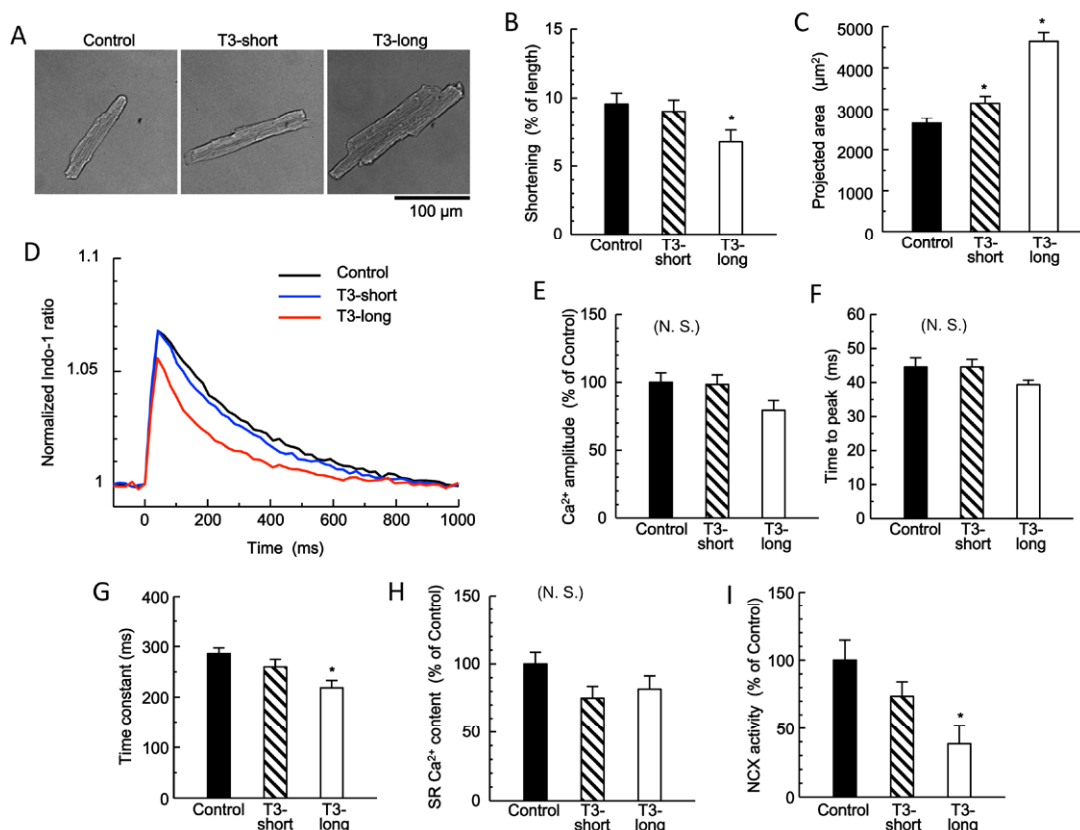


Fig. 3. Effects of T3 on the morphology and function of cardiomyocytes.

(A) Representative images of cardiomyocytes isolated from control, T3-short and T3-long mice.

(B) Cell shortenings of isolated cardiomyocytes electrically stimulated at 1Hz. Control n = 28, T3-short n = 35, T3-long n = 18.

(C) Projected areas of isolated cardiomyocytes.

(D) Averaged traces of Ca<sup>2+</sup> transients in isolated cardiomyocytes electrically stimulated at 1 Hz.

(E) Peak amplitude of electrically evoked Ca<sup>2+</sup> transients.

(F) Time to peak of electrically evoked Ca<sup>2+</sup> transients.

(G) Decay time constant of electrically evoked Ca<sup>2+</sup> transients.

(C)-(G) Control n = 21, T3-short n = 21, T3-long n = 15.

(H) SR Ca<sup>2+</sup> content measured as peak amplitude of caffeine-induced Ca<sup>2+</sup> transients. Control n = 12, T3-short n = 25, T3-long n = 9.

(I) NCX activities in isolated cardiomyocytes. Control n = 16, T3-short n = 25, T3-long n = 10. Values are expressed as means ± SEM. n = number of cells.

altered Ca<sup>2+</sup> handling in cardiomyocytes. In T3-short mice, Ca<sup>2+</sup> transients evoked by electrical stimulations showed no noticeable changes compared with those in the control (Fig. 3D). Although SR Ca<sup>2+</sup> content and NCX activity in T3-short mice were slightly smaller than those in the control mice, there were no significant differences (Fig. 3H and I). In T3-long, the averaged peak amplitude of the electrically-evoked Ca<sup>2+</sup> transients

and SR Ca<sup>2+</sup> content were 79% and 82% of control values, respectively (Fig. 3E and H). Surprisingly, despite an obvious reduction in NCX activity (Fig. 3I), the decay time constant of the Ca<sup>2+</sup> transient in T3-long mice was significantly shortened (Fig. 3G). These results suggest that enhanced SERCA activity is responsible for the increased rate of Ca<sup>2+</sup> removal from the cytosol in T3-long mice.

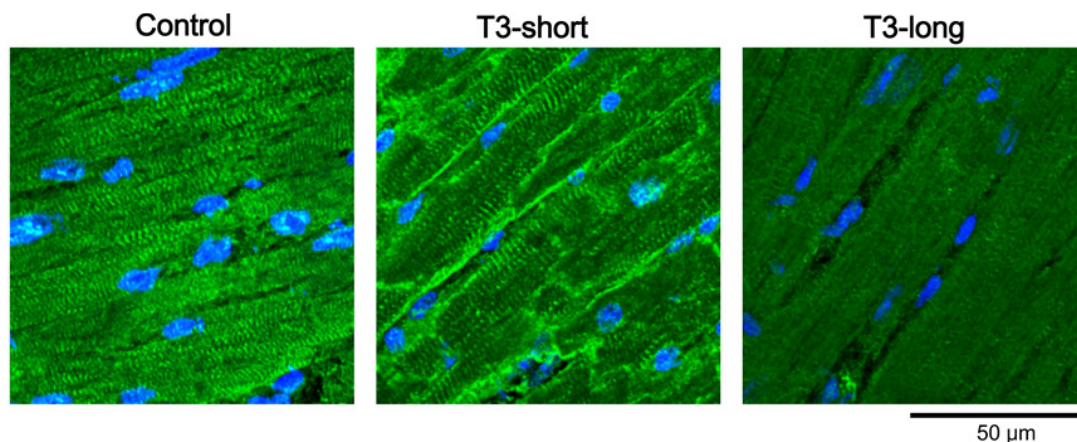


Fig. 4. The changes in the localization of NCX in Control, T3-short and T3-long mice. Double staining with anti-NCX1 antibody (green) and DAPI (blue).

#### Fluorescent immunostaining

Because NCX is mainly localized in T-tubule membranes in the control hearts, immunofluorescent signals of the NCX and ordered patterns appeared (Fig. 4). In mice treated with T3 for a short time, NCX was normally expressed in the control mice. In contrast, the density and regularity of NCX staining were greatly defective in mice treated with T3 for a long time. This suggests that NCX activity significantly decreased.

#### qPCR

As shown in Fig. 5, mRNA expression of the thyroid hormone receptor  $\alpha$  decreased to about 40% of the control level after one week of T3 administration (T3-short), and it recovered to about 50% with long-term administration (T3-long).

## DISCUSSION

We are the first to succeed in evaluating LV contractility using the practically load-independent Ees index in hyperthyroidism at different stages in *in vivo* mice. According to the time-varying elastance model, the elastance of the LV wall increases from an end-diastolic compliant level to end-systolic stiff level (Fig. 6). The increments in elastance can be expressed as a thickened spring

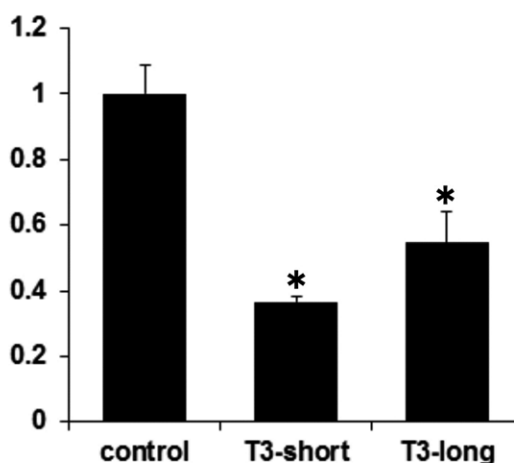


Fig. 5. Total RNA was obtained from adult mouse hearts (control, T3-short and T3-long), reverse-transcribed, and analyzed by quantitative real time PCR for thyroid hormone receptor  $\alpha$ . \*\*  $P < 0.01$  vs. control group by one-way analysis of variance followed by Dunnett's post hoc test. Data were normalized to the control level which was set at 1 and expressed as mean plus SEM.  $n = 6, 3,$  and  $5$  mice for control, T3-short and T3-long, respectively.

during contraction, and the largest value of the ESPVR provides the contractility of LV (Fig. 6)<sup>21)</sup>. Although this index is widely used to evaluate global ventricular contractility in acute experiments, precise application to the chronic experiment, such as hypertrophy caused by mechanical load or drugs, has not been investigated. In the present

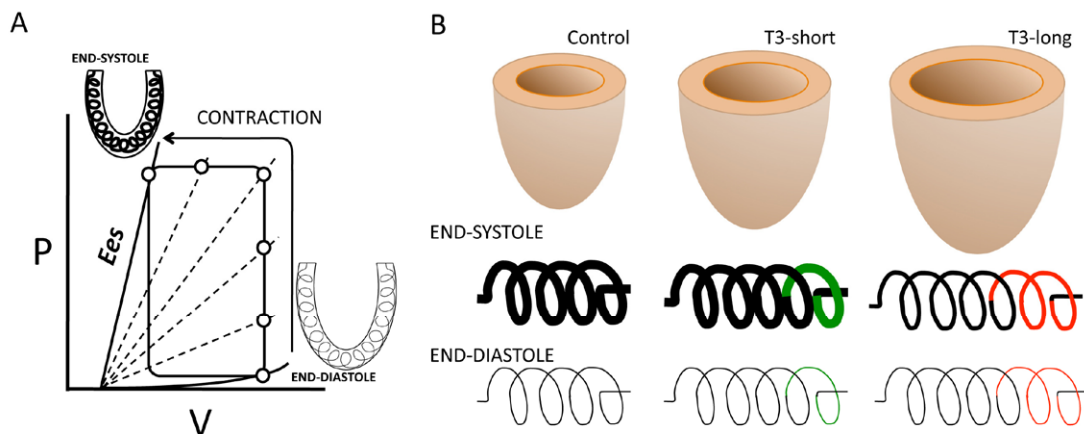


Fig. 6. Interpretations of LV hypertrophy by time-varying elastance model.

(A) Time-varying P-V relation changes its slope as a function of time.  $E_{es}$  (end-systolic elastance) represents cardiac contractility. Schematic left ventricle (LV) includes the spring that increases its elastance during contraction. The elastance of LV wall increases from the end-diastolic compliant level to the end-systolic stiff level.

(B) Schematic LV in control, T3-short, and T3-long (upper), and corresponding conceptual springs in end-systole and end-diastole (lower). The thickness of spring shows its elastance. In T3-short, an additional spring (shown in green) indicates added myocardial tissue by hypertrophic response. The same thickness of spring at end-systole indicates the same contractility per unit myocardium. Although the length of spring increases further in T3-long (shown in red), the thickness of spring decreases indicating that the LV is failing.

study, LV weight increased, but  $E_{es}$  was almost the same as the control in T3-short, indicating that T3 caused LV hypertrophy by adding myocardial tissues that had similar contractile properties to the control heart (Fig. 6). On the other hand,  $E_{es}$  in T3-long was significantly lower compared with the control, indicating that LV contractility per unit LV weight was diminished (Fig. 6). As a result, the hearts in T3-long were failing and showed lower EF compared with the control despite a significant increase in LV weight and lower afterload ( $E_a$ ). If we evaluate the hearts in this model using EF, which is clinically popular but load-dependent, LV in T3-short showed better cardiac function than the control.

Previously, there were two studies that have reported the effects of hyperthyroidism on the heart using  $E_{es}$  or  $E_{max}$  (an index of LV contractility; a synonym of  $E_{es}$ ) in cross-circulated dog and rabbit hearts<sup>22, 23</sup>. Suga H. *et al.* showed that LV contractility indexed by  $E_{max}$  was increased with

an increase of heart rate in dog hyperthyroidism<sup>22</sup>. They also obtained LV oxygen consumption by the measurements of coronary flow and coronary arteriovenous  $O_2$  content difference. Using the framework of pressure-volume area and  $O_2$  consumption ( $Vo_2$ ) relation analysis, which separates  $Vo_2$  for excitation-contraction (E-C) coupling to from total  $Vo_2$  of beating heart<sup>11</sup>, they reported that hyperthyroidism did not increase  $Vo_2$  for E-C coupling and basal metabolism compared with that of euthyroid dog despite LV contractility increasing significantly. They concluded that the  $O_2$  saving effect for E-C coupling in hyperthyroidism was partially due to a myosin isozyme shift from  $V_3$  to  $V_1$ <sup>22</sup>. On the other hand, Goto Y. *et al.* reported that 14 daily *l*-thyroxine administration for rabbits caused cardiac hypertrophy, but the heart rate and  $E_{max}$  were similar for control and hyperthyroid hearts<sup>23</sup> in agreement with our results obtained from mice. Therefore, hyperdynamic state caused by hyperthyroidism seems to be considerably

due to an increase of heart rate and a decrease of arterial resistance. LV contractility of smaller animals with higher spontaneous heart rate seems to be less affected by hyperthyroidism. Another possible reason for the inconsistency of the effects of hyperthyroidism on LV contractility between studies is the dose and duration of thyroid hormone administration.

E-C coupling  $Vo_2$  is primarily due to energy consumption for  $Ca^{2+}$  handling because  $Na^+$  handling energy is negligibly small<sup>11</sup>). In cardiomyocytes, there are two major  $Ca^{2+}$  handling routes that have different molecular  $Ca^{2+}$  ATPase stoichiometries. One is the internal (intracellular)  $Ca^{2+}$  route, including ryanodine receptors that are responsible for the release of  $Ca^{2+}$  from SR and SERCA that sequesters  $Ca^{2+}$  from cytosol into SR. The other is the external (transsarcolmmal)  $Ca^{2+}$  route, including a L-type  $Ca^{2+}$  channel for the influx of  $Ca^{2+}$  and an  $Na^+/Ca^{2+}$  exchanger for the efflux of  $Ca^{2+}$ . In the internal  $Ca^{2+}$  route, SERCA has a  $2Ca^{2+}$  1 ATP stoichiometry of  $Ca^{2+}$  handling via SR<sup>24</sup>). On the other hand, the  $Na^+/Ca^{2+}$  exchanger has a  $3Ca^{2+}$  1 $Na^+$  stoichiometry, and the  $Na^+/K^+$  pump has a  $3Na^+$  1ATP stoichiometry. Therefore, the overall  $Ca^{2+}$  ATPase stoichiometry in the external  $Ca^{2+}$  route eventually becomes 1 $Ca^{2+}$  1ATP<sup>25</sup>). Due to this twofold difference in  $Ca^{2+}$  ATPase stoichiometry, the shift of  $Ca^{2+}$  handling from the internal route to the external route results in the increased  $O_2$  consuming for  $Ca^{2+}$  handling. In the present study, a decrease in NCX and an increase in SERCA expression were observed in hyperthyroidism, indicating that a greater amount of total cytosolic  $Ca^{2+}$  was handled more economically. This is another possible mechanism of the  $O_2$  saving effect for E-C coupling in hyperthyroidism.

In the isolated cardiomyocyte experiments, cell shortening in T3-short was similar to that in the control, and a significant decrease was observed in T3-long. These findings were consistent with

the results of the LV global contractility Ees. The reason why global and cellular contractility were diminished, despite a constancy of peak amplitude of the  $Ca^{2+}$  transients, may be explained by futile  $Ca^{2+}$  cycling and/or a decrease in the  $Ca^{2+}$  sensitivity of myofilaments<sup>26,27</sup>). Fluorescent immunostaining showed that the localization of NCX to T-tubule became unclear in T3-long, indicating that the dysfunction of cooperation between T-tubule and SR could be another mechanism for the depression of LV contractility. As for increased LV relaxation, concomitant effects of decreased NCX activity and increased SERCA activity resulted in a significant shortening of the decay time constant of the  $Ca^{2+}$  transient in T3-long. As for the relation between NCX and heart failure, many studies reported that NCX expression was increased in human heart failure and also animal models of cardiac hypertrophy and heart failure<sup>28,29</sup>). Enhanced NCX expression has been considered as a beneficial compensatory mechanism for improving LV contractility<sup>30</sup>). Therefore, a decrease of NCX expression caused by hyperthyroidism may be detrimental to a long-term maintenance of cardiac function in spite of acute beneficial effects by  $O_2$  saving property for  $Ca^{2+}$  handling in response to an acute increase of mechanical work caused by a decreased arterial resistance and an increased circulating blood volume. To assess whether decreased expression of NCX could be responsible for the progression of heart failure in hyperthyroidism, cardiac specific and drug-inducible overexpression of NCX on hyperthyroid mice will be warranted.

Additionally, we performed qPCR for the thyroid hormone receptor  $\alpha$ , which has been reported to be negatively regulated by the thyroid hormone<sup>31</sup>), to investigate whether the long-term administration of the thyroid hormone affects cardiomyocytes. Administration of T3 halved mRNA expression of thyroid hormone receptor  $\alpha$  both in T3-short and T3-long.

The limitations of the present study are discussed. First, it has been reported that the LV Ees in rats was not always linear but convex superior at a high LV pressure range<sup>32)</sup>. However, we obtained the value of Ees at a lower LV pressure range by performing IVCO; linear regression for Ees showed good correlation and therefore the Ees values are reliable as a contractility index. Second, we could not show the hyperkinetic state caused by the thyroid hormone in LV mechanics experiments. One possible reason is the heart rate, which was kept constant during the measurement. Hyperthyroidism increases the heart rate, resulting in higher LV contractility with an increase in the peak amplitude of the  $\text{Ca}^{2+}$  transients in a conscious state. Third, we kept the heart rate  $500 \pm 20$  beats/min during LV mechanics experiments by controlling the concentration of sevoflurane as described in materials and methods to avoid the effects of heart rate on LV contractility. However, there is a possibility that higher concentration of sevoflurane was needed to control the heart rate in T3-treated groups resulting in a greater suppression of LV contractility compared to control. To assess this possible bias, we performed a chronic recording of electrocardiography on an unrestrained, conscious mouse. The values of the heart rate in control, T3-short, and T3-long were 648, 698, and 719 beats/min, respectively. Increases in the heart rate in T3-treated groups seems to be relatively small ( $\sim 10\%$ ) compared with larger animals that show lower spontaneous heart rate<sup>22)</sup>. Therefore, although the difference of necessary concentrations of sevoflurane among the groups to keep the similar heart rate can be a reason why LV contractility in T3-short was similar to that in control in contrast to earlier studies that show higher LV contractility in acute hyperthyroidism<sup>22)</sup>, this bias can be considered relatively small in mice model.

In conclusion, we succeeded in evaluating LV contractility in hyperthyroid mice by using an

Ees index that is practically load-independent. T3 administration shifted the  $\text{Ca}^{2+}$  route to the  $\text{O}_2$ -saving energetics in the E-C coupling by a decrease in NCX and an increase in SERCA expression. Despite these energy-saving changes, LV contractility was diminished with long-term T3 administration, showing a constancy of the peak amplitude of the  $\text{Ca}^{2+}$  transients and a decrease in NCX activity.

#### ACKNOWLEDGMENTS

The study was partly supported by JSPS KAKENHI Grant Number (23300171, 26282127 and 26703014) and Research Project Grant (26Kiban-81) from Kawasaki Medical School, all of Japan

I appreciate the supervision of this work by Prof. Satoshi Mohri. I also thank to Ken Hashimoto and Yoshihiro Ujihara for their helpful advice. Furthermore, I am grateful for them that taught me the experimental technique.

#### DISCLOSURES

There is no conflict of interest in this study.

#### REFERENCES

- 1) Reed TD, Babu GJ, Ji Y, Zilberman A, Ver Heyen M, Wuytack F, Periasamy M: The expression of SR calcium transport ATPase and the  $\text{Na}^+/\text{Ca}^{2+}$  Exchanger are antithetically regulated during mouse cardiac development and in Hypo/hyperthyroidism. *J Mol Cell Cardiol* 32: 453-464, 2000
- 2) Pantos C, Xinaris C, Mourouzis I, Malliopolou V, Kardami E, Cokkinos DV: Thyroid hormone changes cardiomyocyte shape and geometry via ERK signaling pathway: Potential therapeutic implications in reversing cardiac remodeling? *Molecular and Cellular Biochemistry* 297: 65-72, 2007
- 3) Danzi S, Klein I: Thyroid disease and the cardiovascular system. *Endocrinol Metab Clin North Am* 43: 517-528, 2014
- 4) Ojamaa K: Signaling mechanisms in thyroid hormone-induced cardiac hypertrophy. *Vascul Pharmacol* 52: 113-119, 2010

- 5) Kim BH, Cho KI, Kim SM, Kim N, Han J, Kim JY, Kim JJ: Heart rate reduction with ivabradine prevents thyroid hormone-induced cardiac remodeling in rat. *Heart Vessels* 28: 524-535, 2013
- 6) Sussman MA, Lim HW, Gude N, Taigen T, Olson EN, Robbins J, Colbert MC, Gualberto A, Wieczorek DF, Molkenkin JD: Prevention of cardiac hypertrophy in mice by calcineurin inhibition. *Science* 281: 1690-1963, 1998
- 7) Molkenkin JD, Lu JR, Antos CL, Markham B, Richardson J, Robbins J, Grant SR, Olson EN: A calcineurin-dependent transcriptional pathway for cardiac hypertrophy. *Cell* 93: 215-228, 1998
- 8) Passier R, Zeng H, Frey N, Naya FJ, Nicol RL, McKinsey TA, Overbeek P, Richardson JA, Grant SR, Olson EN: CaM kinase signaling induces cardiac hypertrophy and activates the MEF2 transcription factor in vivo. *J Clin Invest* 110: 1395-1406, 2000
- 9) Park KWI, Dai HB, Ojamaa K, Lowenstein E, Klein I, Sellke FW: The direct vasomotor effect of thyroid hormones on rat skeletal muscle resistance arteries. *Anesth Analg* 85: 734-738, 1997
- 10) Biondi BL, Palmieri EA, Lombardi G, Fazio S: Effects of thyroid hormone on cardiac function: the relative importance of heart rate, loading conditions, and myocardial contractility in the regulation of cardiac performance in human hyperthyroidism. *J Clin Endocrinol Metab* 87: 968-974, 2002
- 11) Suga H: Ventricular energetics. *Physiol Rev* 70: 247-277, 1990
- 12) Sagawa K: The end-systolic pressure-volume relation of the ventricle: definition, modifications and clinical use. *Circulation* 63: 1223-1227, 1981
- 13) Suga H, Yamada O, Goto Y, Igarashi Y: Peak isovolumic pressure-volume relation of puppy left ventricle. *Am J Physiol* 250: H167-172, 1986
- 14) Sunagawa K, Maughan WL, Burkhoff D, Sagawa K: Left ventricular interaction with arterial load studied in isolated canine ventricle. *Am J Physiol* 245: H773-780, 1983
- 15) Matsubara HI, Takaki M, Yasuhara S, Araki J, Suga H: Logistic time constant of isovolumic relaxation pressure-time curve in the canine left ventricle. Better alternative to exponential time constant. *Circulation* 92: 2318-2326, 1995
- 16) Katanosaka YI, Kim B, Wakabayashi S, Matsuoka S, Shigekawa M: Phosphorylation of Na<sup>+</sup>/Ca<sup>2+</sup> exchanger in TAB-induced cardiac hypertrophy. *Ann N Y Acad Sci* 1099: 373-376, 2007
- 17) Shioya T: A simple technique for isolating healthy heart cells from mouse models. *J Physiol Sci* 57: 327-335, 2007
- 18) Katanosaka Y, Iwasaki K, Ujihara Y, *et al.*: TRPV2 is critical for the maintenance of cardiac structure and function in mice. *Nat Commun* 5: 3932, 2014
- 19) Wei FY, Zhou B, Suzuki T, *et al.*: Cdk5rap1-mediated 2-methylthio modification of mitochondrial tRNAs governs protein translation and contributes to myopathy in mice and humans. *Cell. Metab* 21: 428-442, 2015
- 20) Igarashi J, Hashimoto T, Kubota Y, *et al.*: Involvement of S1P1 receptor pathway in angiogenic effects of a novel adenosine-like nucleic acid analog COA-C1 in cultured human vascular endothelial cells. *Pharmacol Res Perspect* 2: e00068, 2014. doi:10.1002/prp2.68.
- 21) Suga H: Cardiac function. Chapter. 5 *In* Pediatric Cardiovascular Medicine. (J.H. Moller, J.I.E. Hoffman, eds). New York, USA, Churchill Livingstone. 2000, pp 65-77
- 22) Suga H, Tanaka N, Ohgoshi Y, Saeki Y, Nakanishi T, Futaki S, Yaku H, Goto Y: Hyperthyroid dog left ventricle has the same oxygen consumption versus pressure-volume area (PVA) relation as euthyroid dog. *Heart Vessels* 6: 71-83, 1991
- 23) Goto Y, Slinker BK, LeWinter MM: Decreased contractile efficiency and increased nonmechanical energy cost in hyperthyroid rabbit heart. Relation between O<sup>2</sup> consumption and systolic pressure-volume area or force-time integral. *Circ Res* 66: 999-1011, 1990
- 24) Alpert NR, Blanchard EM, Mulieri LA: Tension-independent heat in rabbit papillary muscle. *J Physiol* 414: 433-453, 1989
- 25) Reeves JP, Hale CC: The stoichiometry of the cardiac sodium-calcium exchange system. *J Biol Chem* 259: 7733-7739, 1984
- 26) Seed WA, Noble MI, Walker JM, Miller GA, Pidgeon J, Redwood D, Wanless R, Franz MR, Schoettler M, Schaefer J: Relationships between beat-to-beat interval and the strength of contraction in the healthy and diseased human heart. *Circulation* 70: 799-805, 1984
- 27) Shimizu J, Araki J, Mizuno J, *et al.*: A new integrative method to quantify total Ca<sup>2+</sup> handling and futile Ca<sup>2+</sup> cycling in failing hearts. *Am J Physiol* 275: H2325-2333, 1998

- 28) Sipid KR, Volders PG, Vos MA, Verdonck VF: Altered Na/Ca exchange activity in cardiac hypertrophy and heart failure: a new target for therapy? *Cardiovasc Res* 53: 782-805, 2002
- 29) Weber CR, Piacentino V3rd, Houser SR, Bers DM: Dynamic regulation of sodium/calcium exchange function in human heart failure. *Circulation* 108: 2224-2229, 2003
- 30) Reuter H, Pott C, Goldhaber JI, Henderson SA, Philipson KD, Schwinger RH: Na(+)-Ca<sup>2+</sup> exchange in the regulation of cardiac excitation-contraction coupling. *Cardiovasc Res* 67: 198-207, 2005
- 31) Klein I, Danzi S: Thyroid disease and the heart. *Circulation* 116: 1725-1735, 2007
- 32) Lee S, Ohga Y, Tachibana H, Syuu Y, Ito H, Harada M, Suga H, Takaki M: Effects of myosin isozyme shift on curvilinearity of the left ventricular end-systolic pressure-volume relation of In situ rat hearts. *Jpn J Physiol* 48: 445-455, 1998

